Effect of electrode separation in magnetron DC plasma sputtering on grain size of gold coated samples

K. A. Yahya and B. F. Rasheed

Department of Physics, College of Science, Al - Nahrain University, Baghdad, Iraq

E-mail: drkayahya2005@yahoo.com

Abstract

In this work, an experimental research on a low voltage DC magnetron plasma sputtering (0-650) volt is used for coating gold on a glass substrate at a constant pressure of argon gas 0.2 mbar and deposition time of 30 seconds. We focused on the effects of operating conditions for the system such as, electrode separation and sputtering current on coated samples under the influence of magnetic flux. Electron temperature and electrons and ions densities are determined by a cylindrical single Langmuir probe. The results show the sensitivity of electrode separation lead to change the plasma parameters. Furthermore, the surface morphology of gold coated samples at different electrode separation and sputtering current were studied by atomic force microscopy (AFM). The AFM analysis showed that the variation of average grain diameter and average grain height is nonlinear with a minimum value of average grain diameter 90 nm at electrode separation of 4 cm and 30 mA sputtering current.

Key words

DC magnetron sputtering, glow discharge, langmuir probe, gold grain size.

Article info.

Received: Oct. 2017
Accepted: Nov. 2017
Published: Dec. 2017

تأثير المسافة بين الاقطاب في الترذيذ البلازمي المغناطيسي المستمر على حجم حبيبات الذهب المطلية على النماذج

خالد عباس يحيى و بان فيصل رشيد

قسم الفيزياء، كلية العلوم، جامعة النهرين، بغداد، العراق

الخلاصة

بحث عملي في مجال دراسة الترذيذ البلازمي المستمر ذو الفولتيات الواطئة (0-650v) لطلاء حبيبات الذهب على نماذج من مادة الزجاج وتحت ضغط ثابت لغاز الاركون 0.2 mbar و زمن طلاء 30 sec. تركز البحث على دراسة تأثير الظروف التشغيلية للمنظومة على ابعاد الاقطاب وتيار الترذيذ تحت تأثير المجال المغناطيسي. تم تحديد قيم درجات حرارة الالكترونات وكثافة الايونات والالكترونات بطريقة تشخيص البلازما باستخدام مجس لانكمور اسطواني مفرد. أظهرت النتائج تأثير تغيير المسافة بين الاقطاب على اعلومات البلازما. اضافة الى ذلك فقد تمت دراسة خصائص اشكال النماذج المطلية بالذهب مع تغيير المسافة بين الاقطاب باستخدام مجهر القوة الذرية (AFM). ان نتائج تحليلات (AFM) بينت تأثيرات المسافة بين الاقطاب على معدل قطر وارتفاع حبيبات الذهب المطلية وان هذه التغيرات بعلاقة ليست خطية، وان اقل قيمة لمعدل قطر الحبيبة 90 nm عندما كانت المسافة بين الاقطاب 4 cm و تيار ترذيذ 30 mA.

Introduction

Glow discharge sputtering technologies are used in different applications such as, in industrial and medicine for deposition thin film and surface treatment [1-7]. There are different processes in physical vapor deposition (PVD) techniques such as, laser ablation, evaporation and sputtering used for coating sample [1, 8, 9]. Plasma magnetron sputtering is the most popular techniques used for nanotechnologies and coating samples. In this system, denser

confinement plasma for a noble gas is generated by a magnetic placed behind the cathode electrode. This magnetic field is caused for trapping and forced the free electrons with drift motion so that, it leads a higher rate of sputtering [10-12].

For sputtering of semiconductor or insulating and conducting targets, the rf and dc magnetron sputtering sources are used respectively [11-13].

In this work, a dc planar magnetron sputtering source with different electrode separations were investigated to determine the variations on electrical operation discharge, plasma diagnostics and the morphology of gold coater with a glass substrate at a constant argon gas pressure.

Experimental setup

Fig.1 shows a schematic diagram of the experimental setup. The details of the system are mentioned in the reference [14]. The cathode of gold with a diameter of 57 mm and 0.1 mm thickness as a target according to the sputtering purposes. At the center of the cathode electrode a cylindrical permanent magnet is placed to produce a magnetic field. The discharge chamber is evacuated to a base pressure of $1x10^{-2}$ mbar by using tow-stage rotary pump. The argon working pressure, P, is fixed at 0.2 mbar. For discharging the argon gas a DC power supply ((0-800) volt and (0-100) mA) is used.

A single cylindrical Langmuir probe made of tungsten wire of 0.5 mm diameter, and 5 mm length is positioned near the cathode (target) at a distance of 18 mm to characterize the plasma parameters. A DC power supply ((0-100) volt and (0-150) mA) is used in the probe circuit.

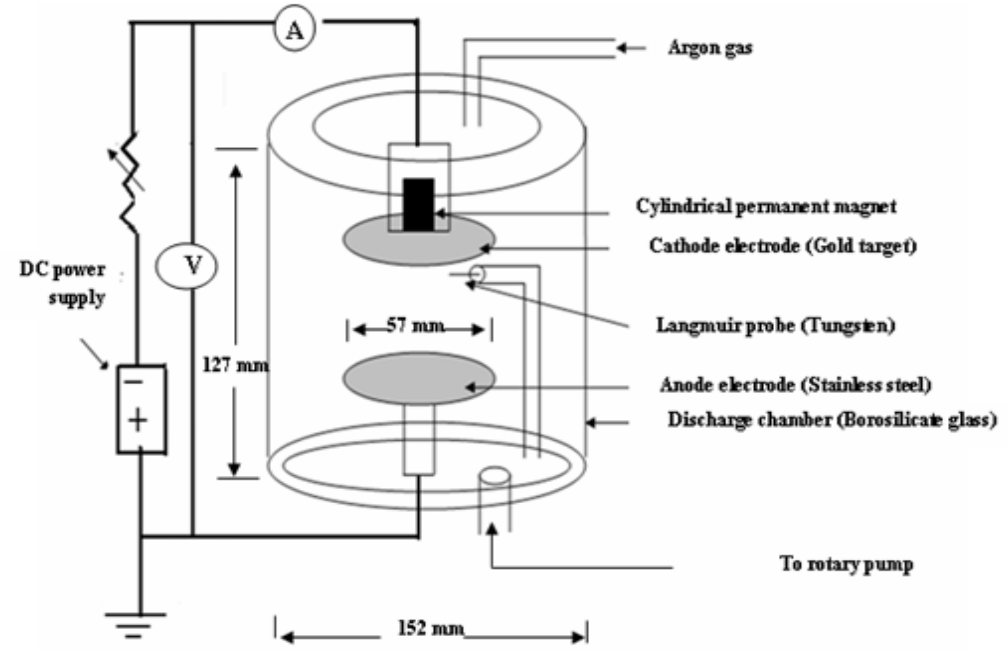

Fig.1: Experimental setup.

Result and discussion

1. Mapping of the magnetic field strengths

In Fig. 2, radial (edge to edge of a cathode) and axial distributions of the magnetic flux B for permanent magnet are mapped by using the Hall probe. The magnetic flux has maximum value of (3350 gauss) in the center cathode region.

2. I-V Characteristics DC argon gas discharge

The I-V characteristics of the discharge at fixed argon gas pressure of 0.2 mbar for different electrode separation, d, of (3, 4, 4.5, 5 and 6) cm are measured as shown in Fig. 3. It is noticed that as the discharge current (sputtering current), I_d, increased the cathode voltage, V_C, increased with variation of the electrode separation.

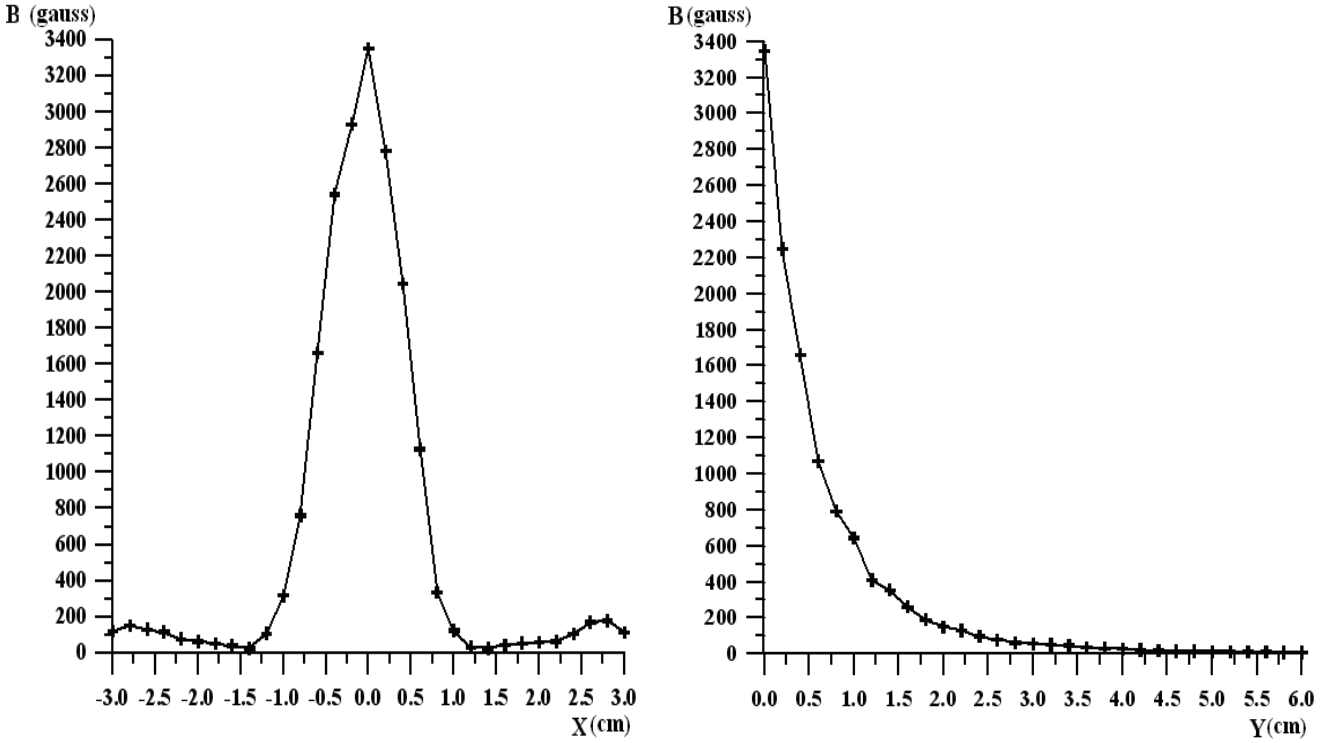

Fig. 2: Mapping of magnetic flux for a- radial distribution. b-axial distribution.

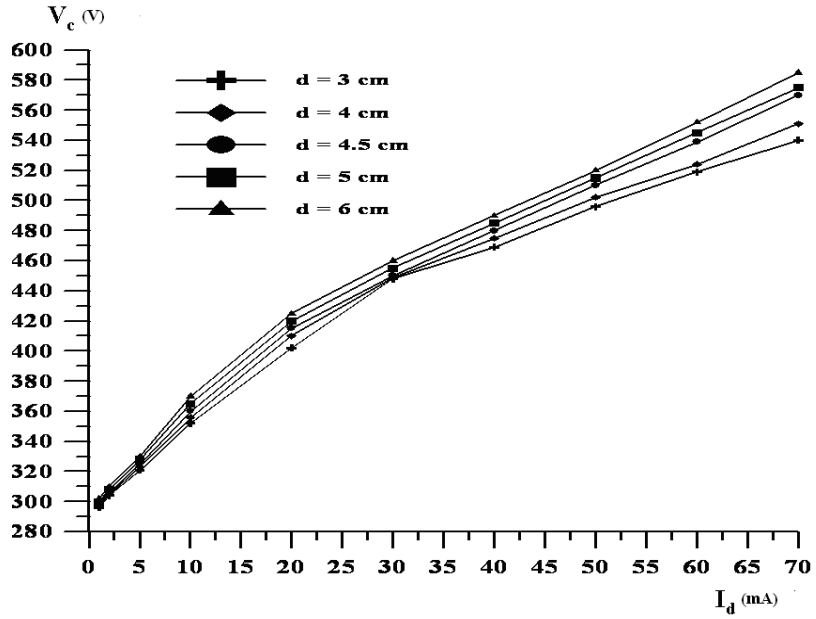

Fig.3: Cathode voltage as a function of sputtering current for different electrode separations at P=0.2 mbar.

3. Plasma parameters

Plasma parameters such as, electron temperature, T_e, density of electrons, n_e, and density of ions, n_i, are very important to describe the behavior of the dc magnetron coater [15, 16]. Also, these parameters are affected by the positive ion flux towards the surface and the morphology of the growing films. In this work, a cylindrical Langmuir probe is used to determine electron temperature and electron and ion densities (see Fig. 1).

Representative probe I-V characteristics are measured for different separations of electrodes at fixed argon gas pressure in the present study.

To avoid the influence of magnetic field on the probe characteristics, one should ensure that [17].

$r_L > r_P$

$$r_L = \left(\frac{\left(\left(\pi m_e k_B T_e \right) / 2 \right)^{1/2}}{e B} \right) \quad (1)$$

where r_P is the probe radius, r_L is the Larmor radius for electron, m_e is the mass of electron, k_B is Boltzmann's constant, T_e is the temperature of electron, e is the charge of electron and B is the magnetic flux. The probe is located at a distance of 18 mm from the cathode surface during experimental studies. As can be seen in Fig. 2 b, the magnetic flux magnitude at this point is equal to 200 Gauss. So, the estimate show it can be neglected the influence of the magnetic on the probe characteristics.

In Fig. 4, the probe I-V curve at d = 3 cm shows that when the probe is negatively biased all electrons are repelled and the ions are accelerated to the probe, with a nearly constant current, called the ion saturation current. As the applied voltage is increased, most high energy electrons are able to travel down the potential gradient to be collected by the probe which acts as electron retarding regime. The temperature of electron, T_e, is calculated from the inverse slope of the logarithmic plot of the electron retarding regime using the equation [18].

$$\frac{d \ln(I_P)}{d \ln(V_P)} = \frac{e}{k_B T_e} \quad (2)$$

where I_P is the probe current and V_P is the probe voltage.

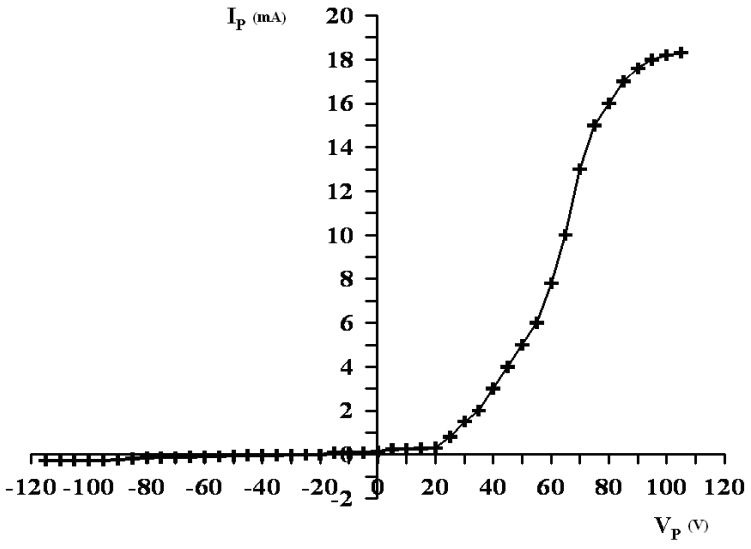

Fig.4: Langmuir probe voltage-current at d= 3 cm, I_d =30 mA and P=0.2 mbar.

In the same way, the temperatures of electrons for different electrode separation are calculated as shown in Fig. 5. It is clear that as the electrode separation increases, more collisions occur and the kinetic energy loss through electron inelastic collisions with atoms increases, thus the electron temperature decreases.

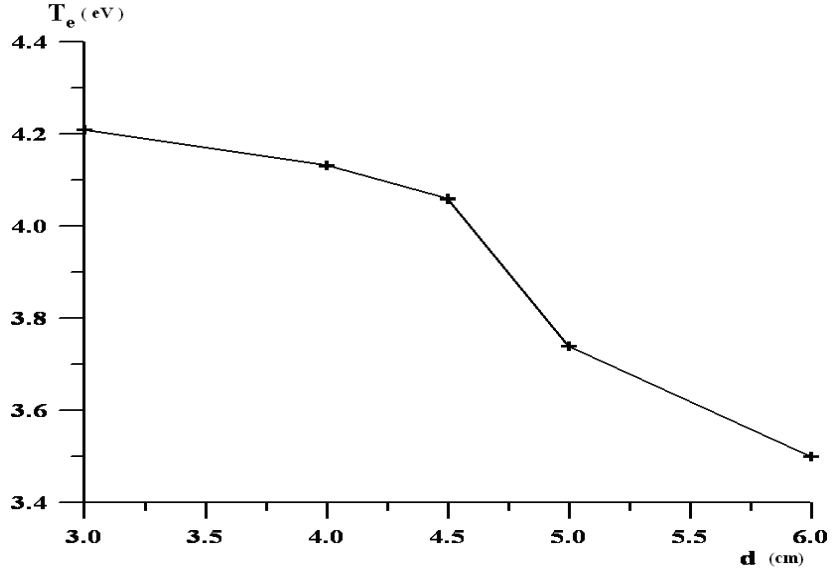

Fig.5: Electron temperature versus electrode separations at I_d=30 mA.

Another plasma parameter which is the electron density, n_e, can be deduced from I-V probe characteristic curve by using the equation [19]

$$(I_e)_{sat} = \frac{1}{4} A_p \, e \, n_e \sqrt{\frac{8 k_B T_e}{\pi m_e}} \qquad (3)$$

where $(I_e)_{sat}$ is the electron saturation current and A_p is the area of the probe. The electron densities for different electrode separations are calculated in Fig.6. It is noticed that the electron densities are increased as the distance d increases. This behavior is due to high energy electrons which are emitted by the cathode and oscillating between repelling potential of the sheaths and the effects of magnetic field, which cause an increase in the ionization of gas atoms by electron confinement electrons leading to a high sputtering rate of target atoms. The ion densities, n_i, for different electrode separation can be calculated based on the orbital motion limit theory (OML) using the equation [17].

$$I_i = A_p \, n_i \, e \frac{\sqrt{2}}{\pi} \left(\frac{-e V_p}{m_i} \right)^{1/2} \qquad (4)$$

where I_i is the ion current, and m_i is the ionic mass (mass of Ar^+ in this study). By calculating the slope of the linear relationship between the square of ion current as a function of probe voltage in the ion saturation region, the ion density is obtained. In Fig.7 the ion density as a function electrode separation is plotted. It is observed that the ion density increased as the electrode separation increases, this due to increase the collisions probability.

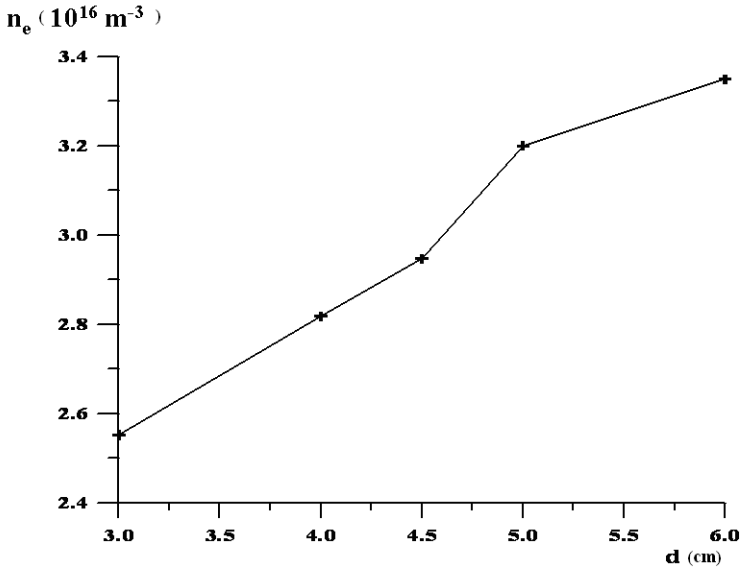

Fig. 6: Electron density versus electrode separation at I_d =30 mA.

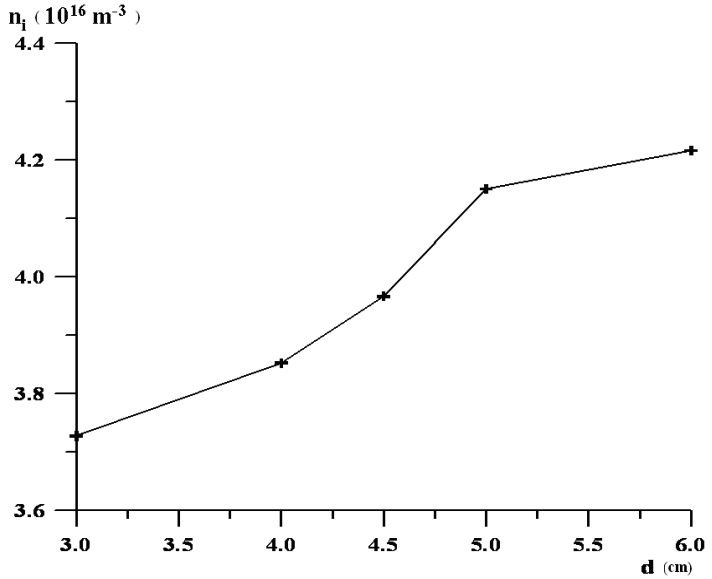

Fig.7: Ion density versus electrode separation at I_d =30 mA.

4. Analysis of gold grain size

In a glass substrate, a series of gold sputtering particles were prepared for different electrode separations, d, at a deposition time of 30 sec. The morphologies for particle's deposition are analyzed by using Atomic Force Microscope (AFM). 3D images from AFM results for different electrode separation at I_d=30 mA are shown in Fig. 8.

The average Au grain diameter, G_d, and average grain height, G_h, as a function of electrode separation for different discharge currents obtained from the analysis of AFM images is presented in Fig. 9. It is shown that, the increase of electrode separation caused increase and decreases in the values of grain diameter and height respectively for different sputtering currents.

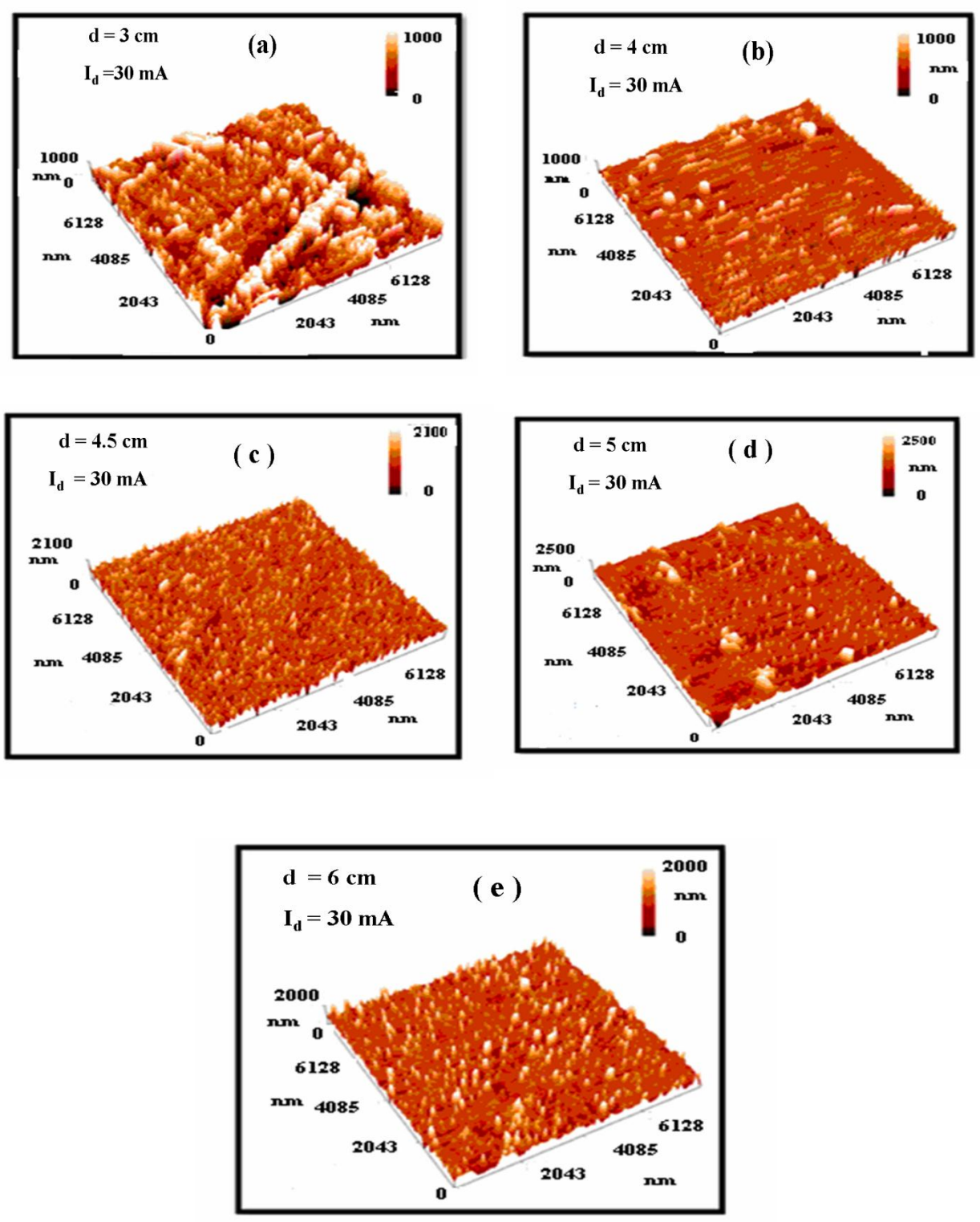

Fig.8: 3D images from AFM results for depositing gold on glass substrate P=0.2 mbar and t = 30 sec for different electrode separations.

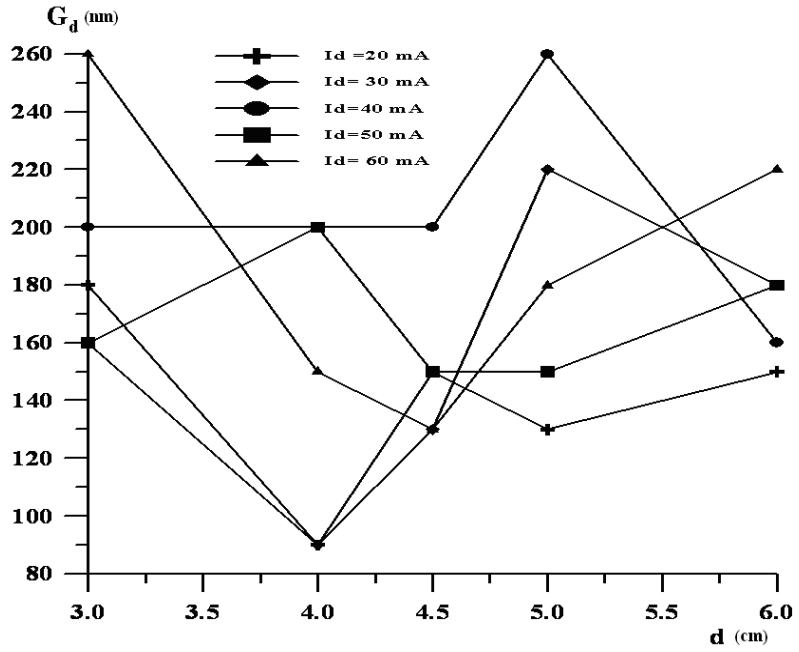

(a)

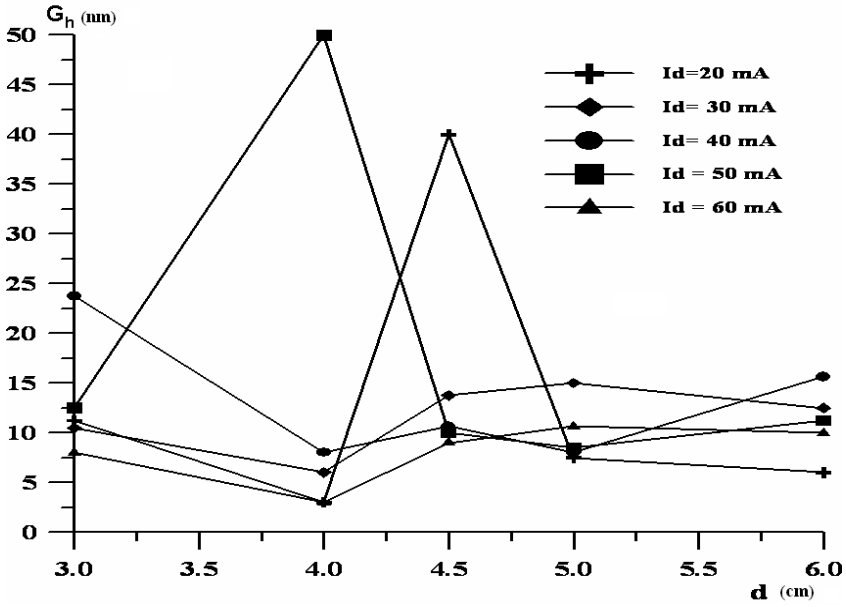

(b)

Fig.9: Effects of variation of sputtering current with electrode separations on a- average gold grain diameter b- average gold grain height.

The average values of maximum and minimum gold grain diameter, G_d, and grain height, G_h, and the values of electron temperatures and ion densities are shown in Table. It is observed that the variation of separation leads to effect on plasma parameters leading to different values for grain diameter and grain height.

Table: Maximum and minimum values for gold average grain diameter, grain height, electron temperatures and ion densities at I_d = 30 mA.

d (cm)	G_d (nm)	G_h(nm)	T_e (eV)	$n_i(m^{-3})$
4	90	6	4.132	$3.8527x10^{16}$
5	220	15	3.74	$4.1512x10^{16}$

Conclusions

The results from the present work, established that the inter-electrode gap and the operational conditions for the system are important parameters, which has a significant impact on the spatial morphology of thin gold coating obtained by sputtering in the magnetron glow discharge. The variation of electrode separation has been found effective for the values of electron and ion temperatures, and electrons densities are sensitive to this separation leads to a change in the surface morphology of samples. Furthermore, the effect of sputtering current is clear from the values of gold grain diameter and grain height. Finally, it is found that the average grain height and grain diameter t with different electrode separations is found to be nonlinear behavior.

References

[1] F.F. Chen, Phys. Plasma, 2 (1995) 2164-2175.
[2] R. B. Heimann, Plasma-Spray Coating Principles and Applications, VCH, Germany, (1996).
[3] A.V. Phelps, Sci. Technol., 10 (2001) 329-343.
[4] M.L. Laroussi, IEEE Trans. Plasma Sci., 30 (2002) 1409-1415.
[5] K. Nygren, M. Samuelsson, A.Flink, H. Ljungcrantz, Å. K. Rudolphi, U. Jansson, Surface and Coatings Technology, 260 (2014) 326-334.
[6] L. Del Giudice, S. Adjam, D. La Grange, O. Banakh, A. Karimi, R. Sanjinés, Surface and Coatings Technology, 295 (2016) 99-106.
[7] J. Wu, B.H. Wu, D.L. Ma, D. Xie, Y.P. Wu, C.Z Chen, Y.T. Li, H. Sun, N. Huang, Y.X. Leng, Surface and Coatings Technology, 315 (2017) 258-267.
[8] J.C. Jao, H.C. Yang, Chinese Journal of Physics, 27 (1989) 169-174.
[9] Y. Bian, M.Liu, G.Ke, Y. Chen, J. DiBattist, E.Chan, Y.Yang, Surface and Coating Technology, 267 (2015) 65-69.
[10] G. Brauer, B. Szyszka, M. Vergohl, R. Bandorf, Vacuum, 84 (2010) 1354-1359.
[11] P.J. Kelly, R.D. Arnell, Vacuum, 56 (2000) 159-172.
[12] S.M. Borah, A.R.Pal, H. Bailung, J. Chutia, Chin. Phys. B, 20 (2011) 014701-1-9.
[13] L.S. Zambom, R.D. Mansano, Journal of Physics, Conference Series, 591 (2015) 012040-1-5.
[14] K.A.Yahya, B.F.Rasheed, Journal of Al-Nahrain University, 19 (2016) 78-85.
[15] P. Saikia, B. Kakati, B.K. Saikia, Physics of Plasma, 20 (2013) 103505-103509.
[16] S. M. Borah, A. R. Pal, H. Bailung, J. Chutia, Applied Surface Science, 254 (2008) 5760-5765.
[17] R. Kar, S.A. Barve, S.B.Singh, D.N. Barve, N. Chand, D.S. Patil, Vacuum, 85 (2010) 151-155.
[18] F.F. Chen, Lecture Notes on Langmuir Probe Diagnostics, Academic, New York, (2003).
[19] D. Bohm, E.H.S. Burhop, H.S.W. Massey, Ed. by A. Guthrie and R.K. Warkerling, M.Graw- Hill, New York, (1949).